

Effect of Displacement Rate on Fracture Toughness of Austenite in Ductile Fracture and Stress Corrosion Cracking at Temperature of 250°C

Anna Brožová, Miroslava Ernestová

Nuclear Research Institute Řež, plc, 250 68 Řež, Czech republic

***Abstract:** The paper describes results of J integral measurement by single specimen method in two environments – non-aggressive and aggressive. In the non-aggressive water the specimens fractured by ductile dimple fracture and the initiation J_i values decrease linearly with logarithm of displacement rate. In aggressive water the presence of stress corrosion cracking further decreased J_i .*

The paper shows micrographs of fracture surface of specimens tested in different test rates and environments.

INTRODUCTION

It is known that fracture toughness of steels is significantly dependent on strain rate [1], mainly in a region of dynamical strain rates. The effect seems to decrease with decreasing strain rates and it is considered practically missing in case of quasi static ones. Standards for the static fracture toughness measurement do not mention the rate influence.

The paper aims to address the strain effect on fracture properties of 08Ch18N12T austenitic steel. It is studied a region of very low strain rates applied at higher temperature of 250°C. In the region a potential strain effect can likely be found due to a combination of very slow mechanical energy input and temperature activation.

The austenitic steel is sensitive to stress corrosion cracking (SCC) only if non-zero positive plastic strain rate is present. The SCC fracture mode is usually transgranular cleavage.

In the paper the fracture toughness measurements in two environments are presented. Results of non-aggressive (non-a.) and aggressive (a.) environments are compared and a possible separation of the strain rate and environmental effects is discussed.

EXPERIMENTAL

Material

The experimental programme was done on the austenitic steel 08Ch18N12T (similar to A321). The chemical composition of the steel is in Tab. 1, the mechanical properties in Tab. 2.

TABLE 1: Chemical composition of the test steel 08Ch18N12T in mass %

Material	C	Mn	Si	P	S	Cr	Ni	Ti	Cu
08Ch18N12T	0.08	1.2	0.7	0.03	0.02	18.4	11.5	0.3-0.7	0.03

TABLE 2: Mechanical properties of the steel 08Ch18N12T at air, room temperature

Material	Yield stress [MPa]	Ultimate tensile stress [MPa]	Elongation [%]	Contraction [%]
08Ch18N12T	299	572	55	68

Specimens 0.5T CT (Compact Tension) were manufactured from the steel; the specimens No. 8,9,11,12,13,16 with side grooves, the specimens No.6,7 without ones. The specimens were pre-cracked by fatigue in air. Pre-cracking sizes are shown in Tab. 3. Pre-fatigue parameters at the last part of the process were $f = 100$ Hz, $K_{\max} = 21$ MPa \sqrt{m} and $R = 0.33$.

TABLE 3: Lengths of pre-cracking in air, room temperature

Specimen No.	6	7	8	9	11	12	13	16
a_0 [mm]	9.85	9.0	9.08	9.07	9.30	9.15	9.81	9.34

Experimental procedure

Fracture toughness measurement tests were carried out using the single specimen J integral method. The same technique was used in non-a. and a. environments.

As non-a. environment it was applied demineralised water without oxygen (dissolved oxygen less than 10 ppb) at 250°C and air at room temperature; as a. environment demineralised water with oxygen (dissolved oxygen higher than 1000 ppb) at 250°C.

The J integral technique used to be employed as an accelerated method for SCC measurement. To determine the threshold value K_{ISCC} of the SCC crack propagation a set of several J integral tests has to be made. The every test has to be carried out by different test rate usually ranging from 100 $\mu\text{m}/\text{hour}$ to 0.1 $\mu\text{m}/\text{hour}$. The threshold value K_{ISCC} is determined from an initiation J_i / K_i versus the displacement rate relationship. The method is standardised and called the rising displacement test (RDT).

The CT specimens were loaded in a constant stroke rate at a hydraulic tensile test machine. In case of high temperature water the specimens were tested inside autoclave vessel. The NRI autoclave system consists of a hydraulic tensile machine and refreshing water loop. The loop supplies water environment to stabilise oxygen content in test chamber. To save test time testing of very low stroke rates (specimens 6, 7 and 12) were carried out by two-step loading; for each step a different stroke rate were applied [2]. Stroke rate is an applied rate of machine. Displacement rates were calculated from measured displacement outside autoclave.

The crack lengths were measured during experiments by the reversed dc potential drop method [3]. In every test data of load, displacement, potential, temperature and pressure were recorded.

The points of crack initiation were determined from record of potential versus load and time. At a first period of test the potential increases only due to a plastic zone formation in front of a pre-crack tip with load increasing. After the crack growth is initiated the potential inclines from a linear relationship on load and time. At the point the initiation factor of stress intensity K_i or J_i was determined.

The J integrals were calculated according recommendation ESIS P1-92.

After test the specimens were final failed by fatigue loading in air and the fracture surface was observed by light and scan electron microscopy.

The average crack growth rates da/dt were calculated from the crack increment divided by test time from the initiation.

Results

Results of experiments are displayed in Tab. 4 and graphs in Figs. 1 - 3.

All the initiation values J_i and $J_{0.2}$ versus displacement rate are plot in Fig.1. There the increasing J_i integral at ductile fracture relationship versus increasing stroke rates in non-a. environment can be seen. The relationship seems to be linear line dependent on logarithm of displacement rate. The J_i values are compared with J_i in a. environment at the same temperature 250°C and completed by measurements in air at room temperature.

TABLE 4: Summary test results

Specimen No.	Environment	Stroke rate [m/s]	Stroke rate [$\mu\text{m}/\text{hod}$]	da* [mm]	da/dt [m/s]	J _i [kN/m]
6	demiwater, 250°C O ₂ > 1000 ppb	2.38E-09	8.7	0.40	1.29E-09	22
7		2.38E-09	8.7	0.03	1.05E-10	12
9	demiwater, 250°C O ₂ < 10 ppb	4.73E-07	1700	4.03	7.96E-07	178
11		4.77E-09	17	4.79	9.03E-09	70
12		8.49E-10	2.4	2.90	1.40E-09	79
8	air, 25°C	1.52E-09	5.5	2.75	1.24E-09	82
13		2.44E-07	870	1.93	1.91E-07	124
16		4.38E-07	1600	1.42	2.88E-07	160

*crack increment during test measured by light microscopy on fracture surface

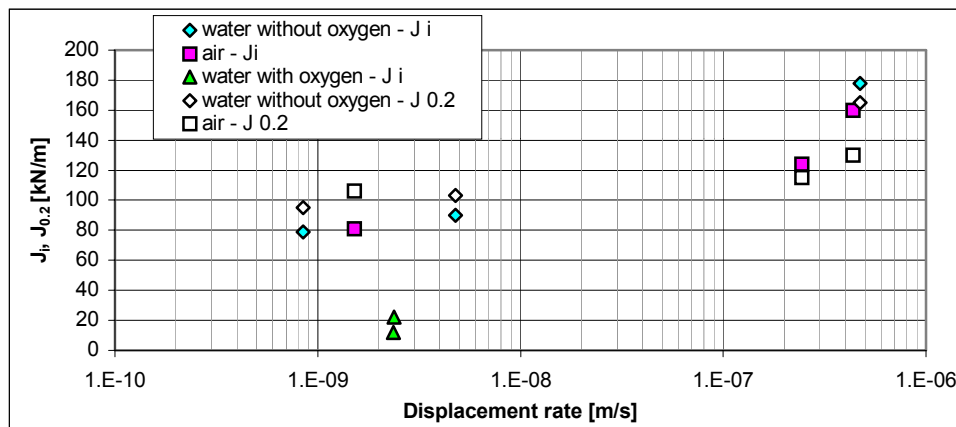


Figure 1: J initiation values – displacement rate relationship

In Fig.2 solid line indicates a linear relationship of the average crack growth rate versus applied displacement rates. Average crack growth rates of specimens 9, 11, 12 versus displacement rate create a linear relationship. Three points of specimens 8, 13, 16 lie below the line because another test machine was used. Two points of specimens 6, 7 are also below it, but due to relatively short crack increment not enough to reach a SCC plateau velocity [4].

Summary of J–R relationships for non-a. and a. environments in Fig. 3 shows J–R curves for all tested stroke rates (ranging from 10⁻⁷ to 10⁻¹⁰ m/s).

Fracture surfaces were observed by SEM. Results of the observations are briefly described in Tab. 5 and micrographs are shown in Figs. 4 – 9.

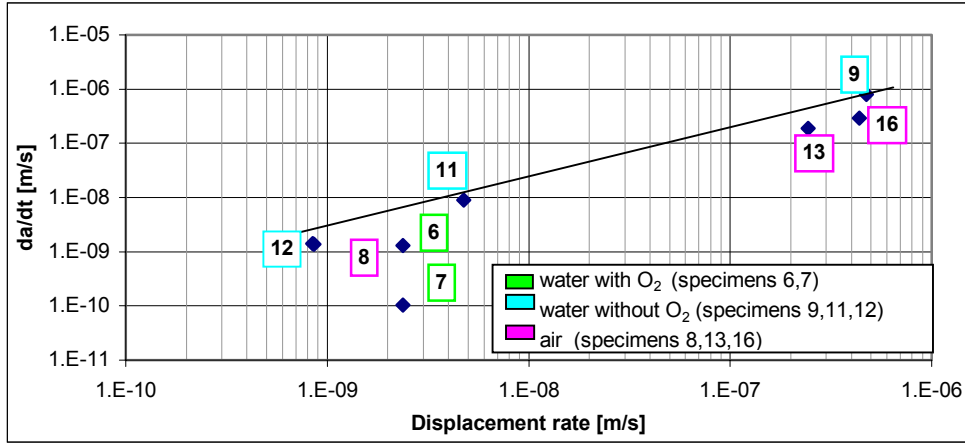


Figure 2: Average crack growth rate - displacement rate relationship

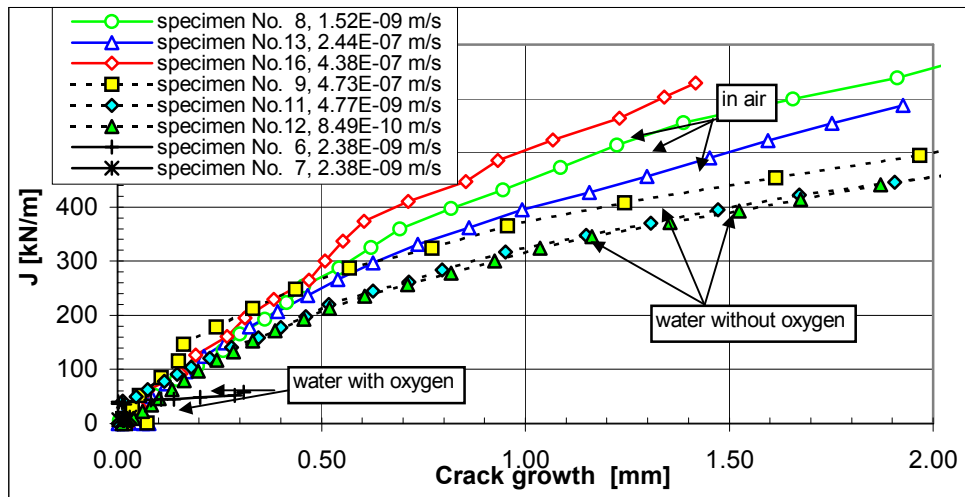


Figure 3: J - R relationship for various stroke rates and environments

TABLE 5: Results of fracture surface observations.

Specimen No.	da [mm]	Fracture appearance
6	0.40*	Quasicleavage, SCC
7	0.03*	Quasicleavage, SCC
9	3.82**	Ductile, dimple fracture, continuous stretch zone, without SCC
11	4.42**	Ductile, dimple fracture, non-continuous stretch zone, without SCC
12	2.71**	Ductile, dimple fracture, non-continuous stretch zone, without SCC

* by light microscopy ** by SEM

Fracture surface of specimens tested in air and in the non-a. environment can be described completely as ductile dimple fracture. Shapes and dimensions of dimples seem to be not slightly changed with decreasing stroke rate (Figs. 4, 5, 6). The dimple shapes of specimen No. 11,12 are lightly more prolonged in comparison with specimen No.9. The stretch zone (SZ) appearance was found slightly dependent on stroke rate. The SZ looked similar to prolonged dimples decorated by slip lines for the highest stroke rate and changed gradually to only slip lines for the slowest ones (Figs. 7, 8).

No environmental effect on the ductile fracture appearance was seen in the non-a. environment. The fracture mode and dimple appearance could be compared to air fracture.

The environmental effect was observed in the a. environment, where a typical stress corrosion crack growth was found. In the both specimens tested in a such environment the fracture mode was characterised as quasi cleavage. The SZ morphology was non homogeneous, the parts of a ductile SZ formation (Fig. 8) alter with the parts of SCC formation (Fig. 9) displayed by secondary crack presence.

DISCUSSION

The measured J – R curves for stroke rates $4.4 \cdot 10^{-7}$ m/s in air and $4.7 \cdot 10^{-7}$ m/s in water without oxygen have very similar course for about the first 0.5 mm of crack increment during the tests. The resulting J_i values for air at room temperature and water without oxygen at 250°C are practically same if usual scatter of 20% of J integral measurement is considered. To support the argument it should be pointed out that two different testing machines were used to the measurement in air and in water. Fracture surface observation confirmed the agreement. It means that no effect of water environment and no effect of higher temperature were measured at the highest stroke rate.

The points of crack growth initiation were determined from potential drop measurements in the both cases ductile fractures and the SCC tests. Due to effect of subjectivity in the process of J_i determination also the standard values, $J_{0.2}$, were evaluated for the specimens with ductile fractures and the values are displayed in the graphs. It is interesting that most of the $J_{0.2}$ values lie very close to or below of the J_i values for the non-a. environment (Fig. 1). It justifies the initiation point evaluation method. Decreasing stroke rate the results of measurements, J_i , also decreased. The relationship is commonly measured at water environments, if the material is

sensitive to SCC. It is very difficult to judge what is the reason for the drop of the initiation stress intensity / fracture resistance, if only mechanical material resistance is responsible of it or if any hidden environmental effect operates.

In case of the non-a. environment used for the test environment in the experimental work we assume that any contribution of the environment to the crack initiation and growth was practically negligible. It was not observed the typical features of the environmental effect manifestations, cleavage fracture or secondary cracks. It was not observed any brittle patterns in fractography.

From the point of view the drop of J_i can be separated to two parts – mechanical and environmental. J_i at the slowest stroke rates first decreased of 50% due to mechanical effect and then of 40% due to the environmental one.

CONCLUSIONS

For the austenitic steel 08Ch18N12T it was measured that the initiation values J_i of resistance to a crack propagation by a stable ductile fracture decrease with decreasing stroke rate ranging from 2.4 to 1700 $\mu\text{m}/\text{hour}$. The J_i value for the slowest stroke rate was determined about 50% of J_i value measured for the highest one, the usual standard J integral test stroke rate. With presence of a corrosion interaction of the a. environment the SCC mechanism appeared on the fracture surface and the initiation J_i values decreased further to about 10% of the J_i value for the usual J-integral test stroke rate.

REFERENCES

1. Kunz, J., (1994) *Základy lomové mechaniky*, ČVUT – FJFI, Praha.
2. Brožová, A. (1997) *Zrychlená zkouška kor. praskání*, Report NRI Řež.
3. Pokluda, J. et all (1994) *Mechanické vlastnosti a struktura pevných látek*, VUT Brno.
4. Brožová, A., Ruščák, M., Dietzel, A.W. (1999) *Proc. 9th Int. Conf. on Environmental Degradation of Materials in Nuclear Power Systems – Water Reactors*, 1-5 August 1999, Newport Beach, CA, USA, Dec. 2000.

Specimen No.9 water without oxygen, the stroke rate $4.73E-07$ m/s

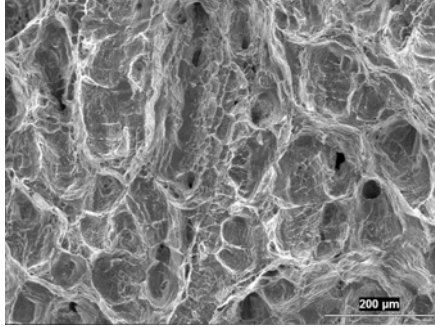


Fig. 4: Crack increment area

Specimen No.11 water without oxygen, the stroke rate $4.77E-09$ m/s

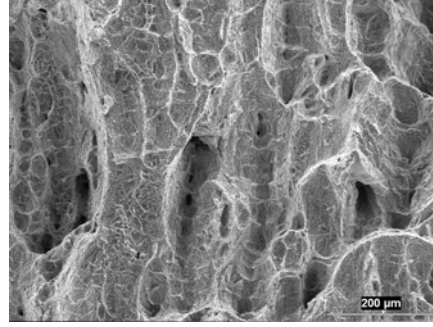


Fig. 5: Crack increment area

Specimen No.12 water without oxygen, the stroke rate $8.49E-10$ m/s

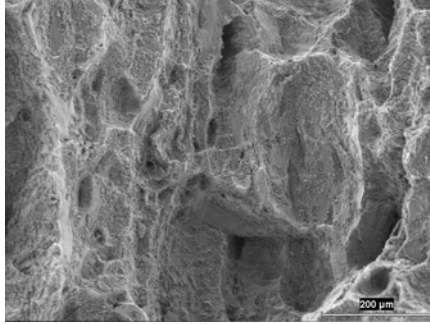


Fig. 6: Crack increment area

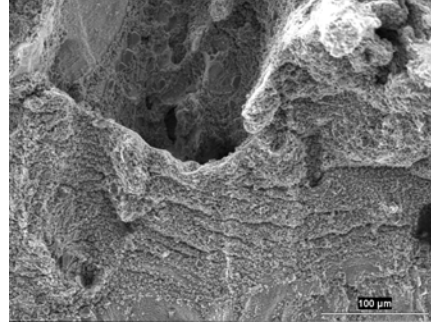


Fig. 7: Crack initiation area:
Pre-fat. in air → stretch zone (SZ) in water
→ ductile dimple fracture
Slip lines on SZ surface

Specimen No.7 water with oxygen, the stroke rate $2.38E-09$ m/s

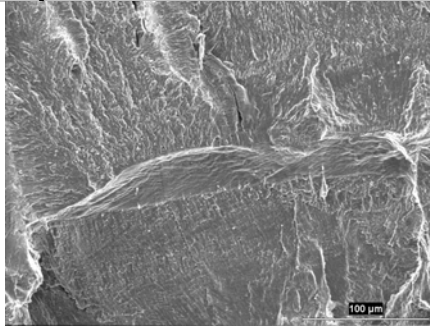


Fig. 8: Ductile stretch zone formation from pre-fatigue crack

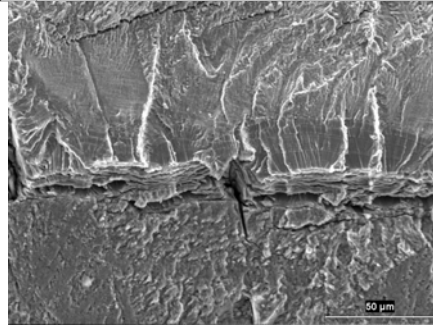


Fig. 9: Another part of crack tip:
Crack initiation from pre-fatigue crack.
Ductile stretch zone + SCC crack increment